Comparison of redox potential dynamics in a diked marsh soil: 1990 to 1993 versus 2011 to 2014

Kristof Dorau[1] and **Tim Mansfeldt**[1]*

[1] Department Geowissenschaften, Bodengeographie/Bodenkunde, Universität zu Köln, Albertus-Magnus-Platz, 50923 Köln, Germany

Abstract

As revealed by an earlier study, young diked marsh soils on the west coast of Schleswig-Holstein (Germany) are characterized by pronounced redox potential (E_H) dynamics. Since soil forming processes occur over a short period of time in these man-made environments, the impact of pedogenesis on E_H was examined by comparing the E_H dynamics measured from November 1989 to October 1993 (weekly measurements) with those measured from November 2010 to October 2014 (hourly measurements) at the same study site in Polder Speicherkoog, Northern Germany. In addition, the necessity for high resolution E_H measurements was assessed as well as the impact of climate change on E_H. Redox potentials were determined in both monitoring campaigns with permanently installed platinum electrodes at 10, 30, 60, 100, and 150 cm soil depths. Soil properties were determined in November 1989 and in August 2013. In 24 years of soil formation, bulk density was demonstrated to increase by 28.5% and 33.3% in 10 and 20 cm depths, respectively, and the sulfide-bearing *Protothionic* horizon lowered from 105 to 135 cm below surface level. Overall, E_H dynamics were similar at all soil depths during both study periods with topsoil compaction not affecting E_H. Annual alterations of E_H were primarily driven by the variable climatic water balance (CWB) and by the corresponding water table (WT) fluctuations. These fluctuations resulted in occasional aeration of the subsoil and subsequent oxidation of sulfides. A forecast of CWB to 2100 predicts an intensified WT drawdown by elevated evapotranspiration rates that should amplify sulfide oxidation. To deduce the soil redox status on a seasonal or annual scale, readings taken at daily intervals are sufficient. To identify biogeochemical processes, it is necessary to monitor E_H on an hourly basis because increases in E_H values of up to 540 mV have been observed within a 24 hour period in temporarily waterlogged horizons.

Key words: marsh soil / monitoring / redox potential (E_H) / pedogenesis / soil heterogeneity

Accepted June 25, 2016

1 Introduction

Determination of the oxidation–reduction (redox) status of a soil and identification of dominant redox processes is of great concern and has been practiced for more than 80 years (*Gillespie*, 1920). Spatial and temporal distributions of reducing conditions in the field can be assessed by installation in the soil of an inert metal electrode (*e.g.*, platinum, Pt) and a reference electrode (*e.g.*, silver/silver chloride, Ag/AgCl). The potential difference between the electrodes can then be determined using a potentiometer to produce readings in mV (*Patrick* et al., 1996). This reading is called the redox potential (E_H) and is a classic measure of reducing soil conditions that affects processes resulting in the release of potent greenhouse gases, controls the mobility of nutrients and pollutants, and alters soil formation. Hence, knowledge of the E_H dynamics in temporarily water saturated soils is important for stakeholders and practitioners, *e.g.*, dealing with the reconstruction of wetlands or to assess associated biogeochemical processes.

Various studies have already dealt with *in situ* monitoring of E_H in field applications, with installation times of up to five years and at various monitoring frequency intervals ranging from hourly to monthly (*DeLaune* et al., 1983; *Faulkner* and *Patrick*, 1992; *Austin* and *Huddleston*, 1999; *Fiedler*, 2000; *Teichert* et al., 2000; *Mansfeldt*, 2003). However, none of these studies integrated the impact of pedogenesis on E_H development. The intensity and development of E_H depends on various time-dependent and external conditions (*Glinski* and *Stepniewski*, 1985). Since these properties (*e.g.*, soil moisture) vary significantly in space and time, the investigation of reducing conditions in soils is a challenge for scientists worldwide. Redox potential measurements using Pt electrodes are at best interpreted as "semi-quantitative expressions of mixed potentials in a non-equilibrium environment" (*Austin* and *Huddleston*, 1999) and therefore, the use of E_H classes over the use of numerical values is encouraged. Soils that undergo frequent changes from oxidizing (E_H > 400 mV) *via* weakly reducing (E_H 400 to 200 mV) and moderately reducing (E_H 200 to –100 mV) to strongly reducing (E_H < –100 mV) soil conditions, and *vice versa*, are located within diked marshes (*Mansfeldt*, 1993, 2003, 2004). In these unique man-made

* Correspondence: T. Mansfeldt; e-mail: tim.mansfeldt@uni-koeln.de

environments, soil-forming processes can be studied over years to decades due to special features of the parent material (*Schroeder* and *Brümmer*, 1969). This contrasts to many other soil environments, *e.g.*, highly weathered soils in tropical regions with low rates of soil formation (*Pillans*, 1997). Diking and drainage of near-surface groundwater plays a crucial role for pedogenetic processes in marshes (*Kuntze*, 1986). These processes comprise (1) compaction and (2) desalination of the topsoil, (3) mineralization of "marine" derived organic matter, and (4) soil acidification by oxidation of sulfide-bearing minerals that is concomitant with the (5) dissolution of carbonate minerals (*Brümmer* et al., 1971; *Müller-Ahlten*, 1994a, 1994b; *Mansfeldt* and *Blume*, 2002). It is expected that climate change will affect these pedogenetic processes and soil properties, but few attempts have been made to evaluate consequences for coastal marsh soils (*Blume* and *Müller-Thomsen*, 2007).

Technical progress in monitoring soil E_H has evolved enormously over the last two decades of data acquisition, especially since electrodes for continuous monitoring of soil E_H have become commercially available to the public (*Vorenhout* et al., 2004). In remote areas (as typified by the present study site), data transmission *via* General Packet Radio Service (GPRS) to a web-based server together with less expensive data storage enables the study of E_H interaction with meteorological and hydrological parameters. As a further advantage, technical improvements with regard to sampling frequency of E_H measurements have made tremendous advancements towards the minute interval (*Shoemaker* et al., 2013). However, little is known about the benefit and advantage of gathering information by performing E_H measurements at a high (*e.g.*, hourly or daily) monitoring frequency interval compared with measurements at a low (*e.g.*, weekly or monthly) monitoring frequency interval.

In this study, manual E_H readings taken on a weekly basis from November 1989 to October 1993 (referred to as hydrological years 1990 to 1993) were compared with automated E_H readings taken on an hourly basis from November 2010 to October 2014 (referred to as hydrological years 2011 to 2014) at Polder Speicherkoog in Schleswig-Holstein, Northern Germany. Each set of readings was obtained from permanently installed Pt electrodes. Soil chemical and physical properties were measured during both monitoring campaigns. The objectives were (1) to assess the impact of pedogenesis (*i.e.*, 24 years of soil formation) on the E_H dynamics; (2) to examine the benefit of E_H measurements on a high frequency basis; and (3) to address the impact of climate change using a forecast of the climatic water balance (CWB) to the year 2100 to evaluate future scenarios for soil pedogenesis and E_H dynamics in these coastal marsh areas.

2 Material and methods

2.1 Study site

The monitoring campaign was carried out at Polder Speicherkoog, situated 30 km north of the river Elbe in Schleswig-Holstein, Northern Germany (54°8'1" N, 8°58'28" E; 0.5 m.a.s.l.). The Polder is part of the Meldorf Bight and was diked in 1978. The monitoring station is 3 km from the shoreline and belongs to a non-cultivated field embedded in an agrarian landscape. At the study site, the typical vegetation consists of willow bushes (*Salix ssp.*), elder bushes (*Sambucus nigra*), and fireweed (*Epilobium angustifolium*) (*Mansfeldt*, 2003). The E_H monitoring was performed in a soil developed from calcareous marine deposits originating from the Dunkirk transgression between 0 to 100 AD (*Hoffmann*, 1991). According to FAO (*IUSS Working Group WRB*, 2014) the soil is a Calcaric Gleysol (Eutric).

2.2 Data collection and soil properties 1990 to 1993

Detailed information about the monitoring campaign from November 1989 to October 1993 is presented in *Mansfeldt* (1993, 2003). Briefly, the monitoring campaign was based on the following approach: E_H was monitored in quintuplicate with permanently installed Pt electrodes at 10, 30, 60, 100, and 150 cm depths on a weekly basis. The Pt electrodes were self-made with a Pt wire (2 mm diameter, 20 mm length) welded on a copper (Cu) wire and connected to a Cu lead. The electrode body was embedded into an acrylic tube (8 mm diameter, variable length, depending on the measurement depth) and coated with a ceramic jacket at the Pt and Cu wire section to prevent intrusion of water (*Pfisterer* and *Gribbohm*, 1989). The Pt electrode cables were labeled at the end and fed into a waterproof container in which E_H readings were taken manually by connecting a portable pH meter to the Cu wire with the support of an alligator clip (*Mansfeldt*, 2003). The water table (WT) depth was measured concomitantly with E_H readings on a weekly basis, within a 200 cm (50 mm diameter) perforated polyvinyl chloride pipe.

A few meters adjacent to the monitoring plot, disturbed and undisturbed soil samples were taken in November 1989 from an excavated soil profile to determine soil physical and chemical properties as follows: soil pH was measured potentiometrically using a glass electrode in a 0.01 mol L^{-1} calcium chloride ($CaCl_2$) solution in twofold repetition. Undisturbed soil samples were taken with steel cylinders (100 cm^3), weighed after saturation within a water bath and weighed again after incubation at 105°C for 24 h to determine soil porosity (pore soil volume per total soil volume) and bulk density (mass of dry soil per unit bulk volume) in eightfold repetition. The grain size distribution was obtained by the sieve and settling method. Total carbon (TC) was determined by dry combustion of the material at 1,200°C (TR 3600 Deltronik). Inorganic carbon (IC) was determined by adding perchloric acid ($HClO_4$; 15%) to the samples, which were preheated to 60°C within the same analyzer to detect CO_2 by Coulomb electrochemical titration. Organic Carbon (OC) was calculated as the difference between TC and IC. Iron oxides (Fe_d) were extracted using dithionite-citrate-bicarbonate (DCB) and the solution analyzed for total iron (Fe) concentrations via flame atomic absorption spectroscopy (*Mansfeldt*, 1994, 2003). Reduced inorganic sulfur (S) was determined on fresh material immediately post-sampling as chromium-reducible S using a distillation apparatus according to *Wieder* et al. (1985). Each of these parameters were determined in twofold repetition.

2.3 Data collection and soil properties 2011 to 2014

The study site was located 10 meters adjacent to that of the initial monitoring campaign. All instruments were installed within a 2 × 2 m plot in March 2010. Readings were stored in a data logger (enviLog Maxi, ecoTech, Bonn, Germany) and transmitted at 8 h intervals to a web-based server *via* GPRS/Internet. Monitoring operations were carried out as follows: soil E_H was measured with permanently installed Pt electrodes (ecoTech, Bonn, Germany) in threefold repetition at 10, 30, 60, 100, and 150 cm monitoring depths. An Ag/AgCl electrode (ecoTech, Bonn, Germany; 3 M KCl internal electrolyte) was placed in a salt bridge to act as the reference electrode in the middle of the measuring plot around which the working electrodes were placed in a stellar configuration. This configuration of the electrodes is nearly the same as that implemented by the initial campaign over 1990 to 1993, with the exception of the smaller-sized Pt tip (1 mm diameter, 10 mm length). The electrode potential was adjusted by adding +207 mV (deviation of the reference electrode against the standard hydrogen electrode) to calculate the E_H. The WT depth was determined in a 2.0-m perforated polyvinyl chloride tube using a relative pressure sensor (PDLR, ecoTech, Bonn, Germany). All measurements and calculations were performed on an hourly basis and converted to daily, weekly, monthly and annual averages or sums. XLSTAT-Pro (Addinsoft V.2014.1.05.) software was used to statistically analyze the dataset.

In August 2013, 24 years after the initial monitoring campaign, disturbed and undisturbed soil samples were taken to evaluate changes in the most important soil chemical and physical properties. The soil pH was measured potentiometrically using a glass electrode in a 0.01 mol L^{-1} $CaCl_2$ solution mixed 5:1 with soil (v/v). In addition, undisturbed soil samples were taken with 250 cm^3 steel cylinders in eightfold repetition per observation depth and saturated in a water bath in the laboratory, and then weighed before and after drying at 105°C for 24 h to calculate the soil bulk density and porosity. Grain size distribution was determined by the sieve and settling method, TC was measured by dry combustion with a CNS analyzer (Vario EL cube, Elementar, Hanau, Germany), IC was measured by dry combustion after adding hydrochloric acid (HCl), and OC determined from the difference between TC and IC. Iron oxides of homogenized and air-dried samples were extracted using dithionite-citrate-bicarbonate (DCB) (*Mehra* and *Jackson*, 1960). The extracts were measured afterwards *via* flame atomic absorption spectroscopy (iCE 3000 series, Thermo Scientific, Waltham, USA). Reduced inorganic S was determined as mentioned above. Replicates of measurements for each parameter were equal to the period from 1990 to 1993.

2.4 Climatic water balance and forecast

For both measuring campaigns, precipitation and meteorological data were taken as a daily sum or mean value from the weather station Cuxhaven (15 km southwards) (*German Meteorological Service*, 2009; *Potsdam Institute for Climate Impact Research*, 2013).

The Haude formula was used to calculate rates of evapotranspiration in mm d^{-1} according to:

$$PET_{Haude} = f \times e_s \left(1 - \frac{F}{100}\right), \quad (1)$$

with f being a plant specific coefficient for grassland (*Loepmeier*, 1994); e_s is the water vapor saturation deficit (hPa) for air at 14:00 CET; and F is the relative humidity (%). The vapor pressure deficit was calculated using the maximum air temperature (T), which is assumed to be equal to the air temperature at 14:00 CET, according to:

$$e_s = 6.11 \times e^{\frac{(17.62T)}{(243.12+T)}}. \quad (2)$$

The climatic water balance (CWB) was calculated as the difference between the monthly sums of precipitation and PET_{Haude}. A forecast of air temperature, relative humidity, and precipitation to 2100, based on the regional climate model STAR (*Orlowsky* et al., 2008; *German Meteorological Service*, 2009; *Potsdam Institute for Climate Impact Research*, 2013) was used to evaluate the possible occurrence of changes, *e.g.*, towards drier summers. Based on the data, the CWB was calculated in the same manner as previously described. Scenarios account for the Representative Concentration Pathways (RCPs) 2.6 and 8.5 that describe the possible range of radiative forcing with 2.6 and 8.5 W m^{-2} proposed by the Intergovernmental Panel on Climate Change.

3 Results

3.1 Soil properties

No significant change of pH values was identified between the two monitoring campaigns (as evident by the two-tailed t-test at the 5% significance level) and a slightly alkaline soil reaction indicates that calcareous material is still present at the study site (Table 1).

Compared with the 1990 to 1993 monitoring campaign, the bulk density increased at depths of 10 and 20 cm by 28.5% and 33.3%, respectively, but remained constant in the subsoil. Accompanying the changes of bulk density, the porosity decreased in these depths from 0.651 cm^3 cm^{-3} to 0.533 cm^3 cm^{-3} and from 0.649 cm^3 cm^{-3} to 0.513 cm^3 cm^{-3}, respectively (Table 1). The porosity decreased slightly at 30 cm, but no change of bulk density and porosity occurred at 60, 100, and 150 cm depths. Clay contents were similar in the topsoil (10 and 20 cm) and the bottom of the soil profile but differed at 30 and 60 cm depths. The OC content gradually decreased from the top 26.5 (28.6) g OC kg^{-1} soil to the bottom 3.7 (2.0) g OC kg^{-1} soil of the soil profile in 1989 (2013), whereas the IC content gradually increased from the top 3.0 (2.1) g IC kg^{-1} soil to the bottom 4.7 (5.7) g IC kg^{-1} soil of the soil profile. These findings demonstrate that over 24 years of soil formation (1989 to 2013), the OC and IC content remained stable over time (Table 1). However, the OC and clay contents were found to be subject to small-scale variations. This is corroborated by the results obtained from the steel

cylinders placed at 60 cm depth during soil sampling in August 2013. A small clay lens originating from a mid-Holocene marine transgression was found to be 2 cm thick and contained elevated OC and clay contents (7.4 g kg^{-1} and 200 g kg^{-1}, respectively) compared with respective values from the surrounding sandy soil in the steel cylinder (2.7 g kg^{-1} and 70 g kg^{-1}) and with the values for 100 cm depth (2.6 g kg^{-1} and 60 g kg^{-1}) (Fig. 1, Table 1).

The DCB-extractable Fe contents were highest in the topsoil and decreased towards the bottom of the soil profile. Depth-dependent differences of Fe_d contents between the two monitoring campaigns are likely to be the result of variations in clay content as indicated by the strong correlation between Fe_d and clay ($r = 0.86$, $p = 0.002$, $n = 8$), since the oxidic Fe fraction of a soil correlates with the clay content (*Cornell* and *Schwertmann*, 2003).

3.2 Climatic water balance and water table depth

Mean annual air temperatures of 8.8°C and precipitation of 805 mm during the reference period from 1961 to 1990, together with cool summers and mild winters, characterize the climate of the Polder Speicherkoog. The CWB ranged between 285 mm and 663 mm during both monitoring campaigns with an above average dry year in 1992 and an above average rainfall year in 1993 for the earlier monitoring campaign. Also, 2014 can be considered as a dry year with significantly higher evapotranspiration rates compared with the reference period (Table 2). According to the climate projection from 2071 to 2100 under the RCP2.6 scenario, the annual CWB remains constant compared with the 30-year reference period from 1961 to 1990, with a slight shift towards drier summers (May to October) (Table 2). This development is intensified under the RCP8.5 scenario with a CWB of only 361 mm y^{-1}, due to a lowering of annual precipitation and enhanced evapotranspiration rates. A decrease of the CWB under this scenario has to be highlighted during the hydrological summer.

Typically for all years, in spring (April to May) the WT decreased because of the partial negative CWB when evapotranspiration exceeded precipitation but increased in early fall (October to November) when the water demand of the vegetation declined and evapotranspiration decreased (Fig. 2). This annual pattern caused seasonal fluctuations of the WT depth from –10 cm in the winter to –200 cm below ground in the summer. The annual cycle of enhanced evapotranspiration (data not shown) from 1990 to 1993 is similar to the development from 2011 to 2014, but the CWB varied significantly for individual months between both periods. For instance, the dry summer of 1992 with a CWB

Table 1: Selected soil properties in the E_H measurement depth of the monitoring campaign from 1990 to 1993 and from 2011 to 2014 with the corresponding standard deviation. The two monitoring sites were within 10 m of each other.

	Sampling 1989							Sampling 2013						
Soil depth	pH[a]	Bulk density	Porosity	Clay	OC[b]	TIC[c]	Fe_d[d]	pH	Bulk density	Porosity	Clay	OC	IC	Fe_d
/ cm		/ g cm^{-3}	/ cm^3 cm^{-3}	/ g kg^{-1}					/ g cm^{-3}	/ cm^3 cm^{-3}	/ g kg^{-1}			
10	7.0 ± 0.1	0.84 ± 0.12	0.651 ± 0.078	260 ± 5.9	26.5 ± 0.89	3.0 ± 0.87	8.77 ± 0.19	7.1 ± 0.1	1.08 ± 0.03	0.533 ± 0.005	250 ± 0.5	28.6 ± 0.92	2.1 ± 1.31	8.22 ± 0.07
20	7.1 ± 0.1	0.87 ± 0.14	0.649 ± 0.091	250 ± 4.0	19.5 ± 1.01	3.5 ± 0.77	11.90 ± 0.07	7.3 ± 0.1	1.16 ± 0.01	0.513 ± 0.007	210 ± 8.0	17.5 ± 0.11	4.6 ± 0.55	8.23 ± 0.09
30	7.2 ± 0.1	1.29 ± 0.22	0.520 ± 0.051	80 ± 1.5	9.0 ± 0.23	4.5 ± 0.23	3.12 ± 0.07	7.4 ± 0.1	1.29 ± 0.02	0.467 ± 0.013	220 ± 16	9.7 ± 0.47	5.0 ± 0.50	5.11 ± 0.12
60	7.3 ± 0.1	1.43 ± 0.17	0.456 ± 0.032	30 ± 2.0	7.2 ± 0.09	5.7 ± 0.31	0.85 ± 0.05	7.4 ± 0.1	1.41 ± 0.03	0.450 ± 0.001	110 ± 1.5	4.6 ± 0.01	5.9 ± 0.19	1.92 ± 0.02
100	7.3 ± 0.1	1.42 ± 0.11	0.420 ± 0.046	40 ± 1.3	2.8 ± 0.12	5.1 ± 0.36	1.65 ± 0.23	7.6 ± 0.1	1.54 ± 0.02	0.446 ± 0.015	60 ± 2.0	2.6 ± 0.11	5.5 ± 0.12	1.54 ± 0.03
150	7.3 ± 0.1	1.41 ± 0.14	0.468 ± 0.023	90 ± 2.3	3.7 ± 0.19	4.7 ± 0.67	1.45 ± 0.11	7.6 ± 0.1	1.54 ± 0.01	0.435 ± 0.008	50 ± 2.0	2.0 ± 0.01	5.7 ± 0.04	0.95 ± 0.06
60[f]	no clay lens present							7.5 ± 0.1	–	–	200 ± 4.9	7.4 ± 0.17	5.5 ± 0.38	2.48 ± 0.05
60[g]	–[e]	–	–	–	–	–	–	7.5 ± 0.1	–	–	70 ± 2.1	2.7 ± 0.28	4.5 ± 0.27	1.03 ± 0.01

[a] 0.01 M $CaCl_2$ (1:5 ratio).
[b] Organic Carbon.
[c] Inorganic Carbon.
[d] Dithionite-citrate-bicarbonate extractable Fe.
[e] "–" not determined.
[f] Clay lens at 60 cm monitoring depth in 2013.
[g] Sandy material at 60 cm monitoring depth in 2013.

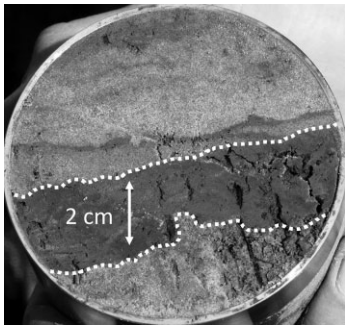

Figure 1: Soil core taken in August 2013 at 60 cm depth within an oximorphic soil horizon. The dashed white line indicates a clay lens originating from mid-Holocene marine transgression.

of –81 mm in June (Fig. 2a) differed remarkably from the moist and mild conditions with 63 mm in June 2013 (Fig. 2c). The impact of water deficiency indicated by the long-lasting dry period from June to September 1992 favored a more intense WT drawdown that remained at lower than –200 cm below ground for a 4-month period (Fig. 2b). In contrast, the mean WT depth remained at –126 cm below ground for the corresponding period in 2013 (Fig. 2d).

3.3 Soil redox potentials

Figures 3a to 3e illustrate the E_H dynamics during the initial campaign. Mean E_H values ranged from 547 mV at 10 cm to –84 mV at 150 cm (Fig. 3, Table 3). The soil was oxidized at the 10 cm monitoring depth throughout the study period (E_H > 400 mV). Variations of E_H occurred at 30 cm with distinct patterns characteristic of oxidizing soil conditions in the summer, to weakly reducing soil conditions in the winter (Fig. 3b). This pattern was even more pronounced at monitoring depths of 60 cm and 100 cm on an annual basis. At 100 cm (150 cm), the redox status was at moderately (strongly) reducing soil conditions for 80% (71%) of the time, but increased in the summer of 1992 to weakly reducing conditions (Fig. 3d, e, Table 3).

From 2011 to 2014, mean E_H values were in the range of 573 mV to –184 mV (Table 3). Oxidizing soil conditions prevailed at 10 cm depth throughout the study period and annual E_H fluctuations at 30, 60, and 100 cm monitoring depths approximate the fluctuations of the initial monitoring campaign. A high standard deviation revealed differences of the E_H readings between individual electrodes from November 2010 to April 2011 at 60 cm depth (Fig. 3h) with differences ranging from strongly to weakly reducing soil conditions. Strongly reducing soil conditions prevailed throughout the study period at 150 cm. The standard deviations were significantly lower at 10 and 150 cm depths compared to the soil depths at 30, 60, and 100 cm, respectively (Table 3). Overall, the soil profile can be separated into an oxidized horizon (10 cm), a predominantly oxidized horizon with seasonal reducing conditions (30 cm), an intermittent reduced horizon with strong seasonal

Table 2: Annual sums of precipitation, evapotranspiration, climatic water balance and mean annual water table depth of the monitoring campaigns during the hydrological years 1990 to 1993 and 2011 to 2014 (hydrological year is from November 01 to October 31). In addition, normal climatic conditions for the periods from 1961 to 1990 and 2071 to 2100 are presented for comparison. The future scenarios account for an anthropogenic radiative forcing of 2.6 W m^{-2} and 8.5 W m^{-2}.

Year	Precipitation / mm y^{-1}	PET_{Haude}[a]	CWB[b]	WT[c] depth / cm below ground
1961 to 1990	805	269	536 (325[d]/209[e])	–
1990	831	295	535	–75
1991	797	293	503	–69
1992	657	372	285	–102
1993	952	289	663	–92
2011	833	310	523	–68
2012	871	285	586	–67
2013	778	258	520	–73
2014	752	356	396	–91
2071 to 2100 (RCP2.6[f])	860	321	539 (348/191)	–
2071 to 2100 (RCP8.5[g])	755	394	361 (274/87)	–

[a]Evapotranspiration according to Haude.
[b]Climatic water balance.
[c]Water table.
[d]Hydrological winter (November, 1 to April, 30).
[e]Hydrological summer (May, 1 to October, 31).
[f]Representative Concentration Pathways with a radiative forcing of 2.6 W m^{-2}.
[g]Representative Concentration Pathways with a radiative forcing of 8.5 W m^{-2}.

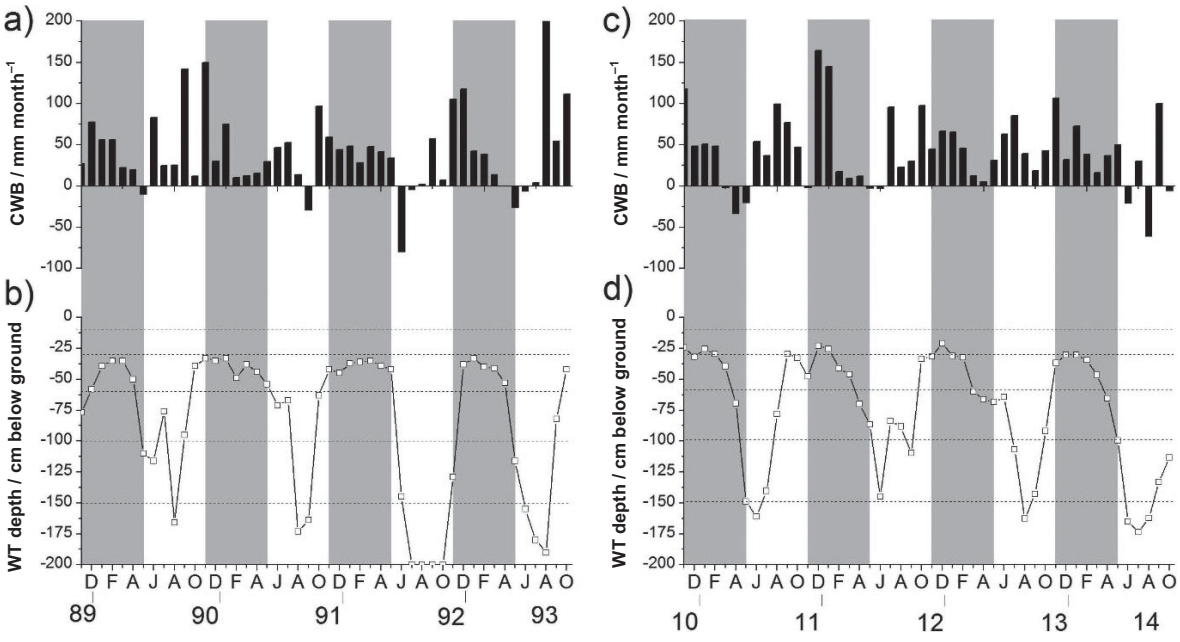

Figure 2: Dynamics of the monthly climatic water balance (CWB) and water table (WT) depth during the hydrological years 1990 to 1993 (a and b) and 2011 to 2014 (c and d). The dashed lines (b and d) indicate the E_H recording depths at 10, 30, 60, 100 and 150 cm depths and the shaded areas indicate the period from November to April (grey) and from May to October (white) of each hydrological year.

variations (60 and 100 cm), and a permanently reduced horizon (150 cm).

The E_H data for both monitoring campaigns were very similar at a monitoring depth of 10 cm (Table 3) in accordance with the E_H dynamics (Fig. 3a, f, Table 3). Although the mean E_H and the standard deviation were very similar at 60 cm during both campaigns (Table 3), the monthly standard deviation was different and more pronounced during the hydrologic winters from 2011 to 2014 (Fig. 3c, h). During the initial campaign, E_H at 30 cm and 100 cm depths remained at a lower level, expressed by differences in mean E_H values of 430 mV to 573 mV and 116 mV to 341 mV, respectively (Table 3). Until June 1992, E_H levels at 150 cm were identical for both monitoring campaigns with an E_H of –161 mV to –184 mV. However, the E_H increase in June 1992 resulted in significant differences for the selected statistical parameters (Fig. 3e, j, Table 3; proven by the two-tailed t-test at the 5% significance level).

3.4 Temporal resolution of redox potential measurements

To assess the possible necessity and benefit resulting from high-resolution E_H measurements, the following program of investigation was undertaken. For the campaign from 2011 to 2014, hourly E_H readings were compared with those obtained at a daily, weekly, and monthly interval by examining their redox class distribution. Arbitrarily, for the daily data, the E_H measured at 8 am of each day was chosen, for the weekly data, the E_H measured at 8 am of each Monday of the week, and for the monthly data the E_H measured at 8 am of each first Monday of the month. Since E_H fluctuations are subject to different time scales (*Fiedler* et al., 2007), the dataset was analyzed for the total period (hydrologic years 2011 to 2014), a seasonal period (hydrologic summer 2011) and an event-based period (July and August 2012) (Fig. 4).

For the total, seasonal, and event-based periods, no significant differences in the redox class distribution were apparent between hourly and daily measurement intervals across all depths. This was also valid at 10, 30, and 150 cm monitoring depths when weekly and monthly readings are given additional consideration. In contrast, at 60 and 100 cm, the redox class distribution differed between the hourly and daily interval, and the weekly and monthly interval. A lowering of the measurement interval resulted in a faulty description of the redox class distribution, considering hourly readings as the 'true' representation of the E_H dynamics for the corresponding periods.

To obtain an insight into the temporal variability of the E_H, we checked for the whole study period the E_H of the single electrodes in the 60-cm depth which revealed the largest oscillations in E_H. Figure 5 displays such an example of the E_H dynamics by illustrating the response of the Pt electrode to aeration as a function of declining WT. E_H started to rise from –90 mV at 1 am towards 450 mV at 12 am and over a 24 h period achieved a range of 540 mV. The E_H increase for this period amounts to 22.5 mV h^{-1} exemplifying short-term fluctuations.

4 Discussion

4.1 Comparison of E_H data and soil properties

Despite the fact that E_H measurements are subject to several limitations (*Ponnamperuma*, 1972), numerous publications

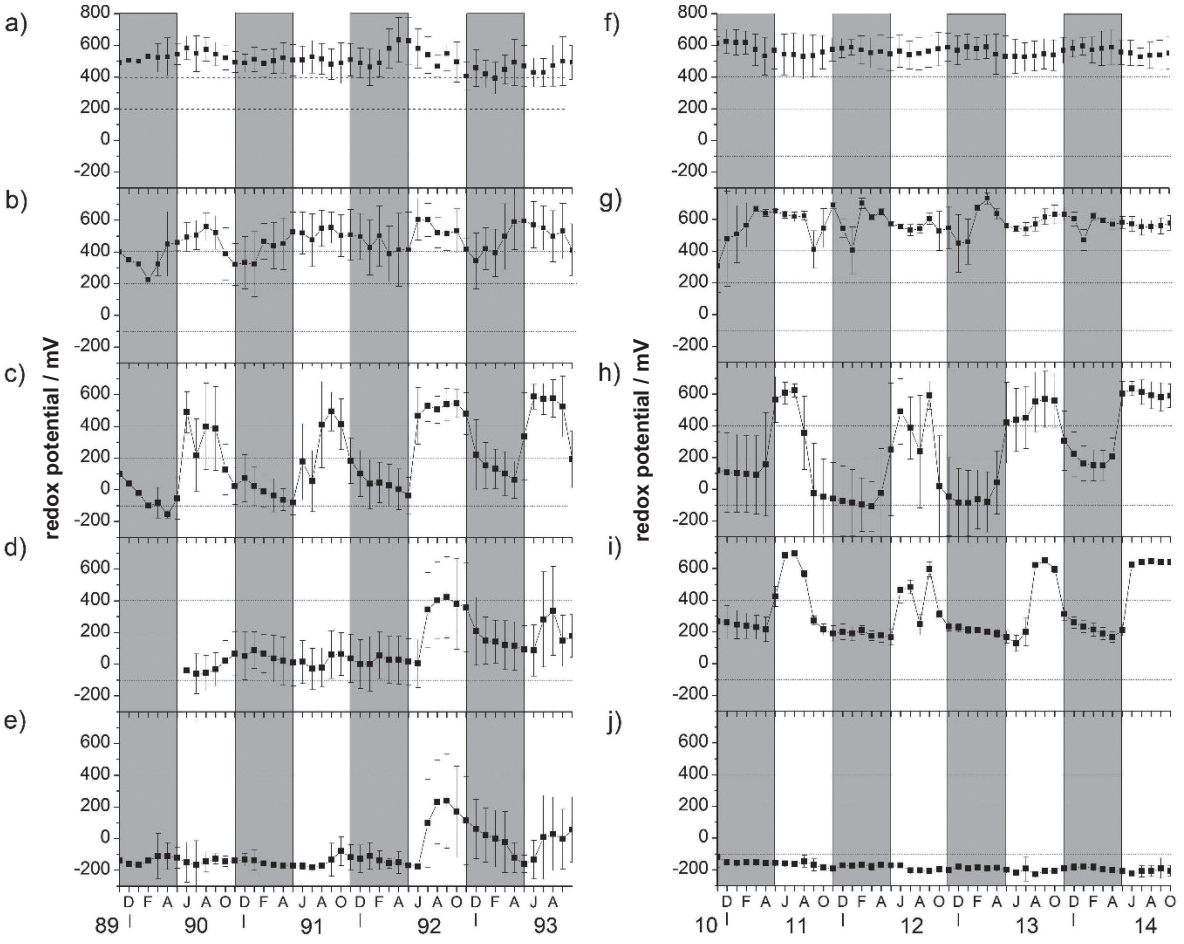

Figure 3: Dynamics of redox potentials (E_H) during the hydrological years 1990 to 1993 (a to e) and 2011 to 2014 (f to j) at 10, 30, 60, 100 and 150 cm depths, respectively. The dashed lines indicate the redox classes of oxidizing (> 400 mV), weakly reducing (400 mV to 200 mV), moderately reducing (200 mV to –100 mV), and strongly reducing (< –100 mV) soil conditions according to *Zhi-Guang* (1985). The E_H dynamics are presented as monthly means with the corresponding standard deviation for measurements in quintuplicate on weekly basis for the initial monitoring campaign and in triplicate on hourly basis for the latter.

have already demonstrated the linkage to abiotic processes, such as aeration (*Mansfeldt*, 2003) as well as the specific impact of redox classes on distinct soil processes (*Yu* et al., 2001). The maximum WT rise (data not shown) was above the 10 cm monitoring depth during both monitoring campaigns, but did not facilitate reducing conditions. It was not possible to assess any impact of the capillary fringe on stimulating the onset of reducing conditions in the topsoil. Hence, oxygen (O_2) replenishment *via* diffusion from the atmosphere was demonstrated as sufficient and exceeded O_2 consumption (Fig. 3a, f). Diking (in 1978) and drainage favored a lowering of WT depths within the Polder Speicherkoog that subsequently conformed to unsaturated soil conditions in the topsoil. An increase of the bulk density, with a decrease of the air-filled porosity at 10, 20, and 30 cm depths (Table 1) verified the process of compaction from 1989 onwards. *Reszkowska* et al. (2011) concluded that a decrease of the air-filled porosity, along with a decrease of the air-conductivity, hampers aeration of the soil. These conditions lead to lowered pathways for gas transport with existing O_2 consumption mediated by existing microbial and root-based mechanisms. However, no assessment was made of any impact on E_H development at these depths or on the subsoil (*i.e.*, at depths of 60, 100, and 150 cm). The annual E_H pattern, with reducing soil conditions in the winter and oxidizing soil conditions in the summer is evident for both study periods at 30, 60, and 100 cm monitoring depths and is related to phases of water saturation caused by the setting of the WT. To achieve oxidizing conditions, it takes on average 4, 10, and 11 d after the WT declined underneath the corresponding E_H measurement depth in 30, 60, and 100 cm depth for the study period from 2011 to 2014. Furthermore, the position of the WT to facilitate oxidizing conditions in these measurement depths was at –33, –75, and –137 cm below ground, respectively. Both results indicate that it takes longer to facilitate oxidizing soil conditions with decreasing soil depth because of microbial and root mediated O_2 consumption during the transport from the atmosphere to the Pt electrode. Besides this biotic process, gas transport over a longer distance through a porous system will take more time than over a shorter distance, which is also reflected by the data. The absence of E_H fluctuations at 100 cm depth from June 1990 to May 1992 can be explained by this process (Fig. 3d), even though the WT was below this depth for a short period (Fig. 2b). It has not been possible to

assess the relationship between a response of the Pt electrode to aeration and the setting of the WT for the period from 1990 to 1993 because of the coarse measurement interval.

In contrast to the period from 2011 to 2014, in which strongly reducing conditions continuously occurred at 150 cm depths, there was a significant increase of E_H, especially during July to September 1992, but also during July to October 1993 (Fig. 3e, Table 3). Such a change in the redox conditions of the subsoil should have influenced black colored Fe(II) sulfide minerals (FeS). The presence of these minerals is a heritage of the Wadden Sea and originates from sulfate (SO_4^{2-}) reduction. Sulfate is abundant in interstitial seawater and with divalent Fe forms various FeS minerals, giving the former Wadden Sea sediments the typical black coloring. These minerals are very sensitive to oxidation. Aeration of deeper soil horizons is associated with the construction of dikes from 1978 and the corresponding drainage for agricultural purposes and with declining WT in the summer time. Consideration of these processes has led to the following proposed sequence of events: (1) O_2 diffusion into deeper soil depths, (2) oxidation of insoluble black-colored sulfide to soluble SO_4^{2-}, (3) translocation of SO_4^{2-} downwards to the WT and its subsequent removal via groundwater from the soil profile, and (4) change of color leaving greyish soil particles behind. Whereas the sulfide-bearing *Protothionic* soil horizon (*IUSS Working Group WRB*, 2014) (*Gr* horizon according to the German soil classification; *AG Boden*, 2005) was closer to the soil surface before diking and drainage, *i.e.*, at –105 cm below ground in November 1989 (11 years after diking), this has declined to –135 cm in August 2013 (35 years after diking). This observation corresponds to a FeS oxidation rate of 1.3 cm y^{-1}. A reduction of monosulfidic S at a depth of 150 cm from 275 mg S^{2-}-S kg^{-1} (1989) to 112 mg S^{2-}-S kg^{-1} (2013) also underlines these pedogenetic processes of diminishing FeS concentrations as a result of prolonged periods of aeration.

Under reducing conditions, major discrepancies between monthly E_H measurements for individual Pt electrodes were evident at 60 cm from 2011 to 2014, contrary to the former campaign where the standard deviation was less pronounced (Fig. 3c, h). It is assumed that the clay lens in Fig. 1 is responsible for this pattern. Higher OC and clay contents presumably caused stronger reducing conditions around the Pt electrode (as a result of higher microbial activity and soil moisture), supporting the assumption that one out of three Pt tips dips into the clay lens and, in general, causes strongly reducing soil conditions (Fig. 3h). In this regard, a continuous placement of Pt electrodes in the soil is encouraged because frequent manual installation and de-installation of electrodes, even when care is taken that the electrodes are placed at the same monitoring depth, can lead to measurements reflecting soil heterogeneity which will be reflected over time.

4.2 Measurement interval of redox potential

Various studies have demonstrated the variability of E_H over small distances (*Yang* et al., 2006). In addition, redox conditions are known to be heterogeneous on a temporal scale and therefore manual measurements performed over discrete time intervals may not be able to capture the 'true' redox dy-

Table 3: Comparison of selected statistical redox potential (E_H) data and distribution of redox classes between the monitoring campaigns from 1990 to 1993 and from 2011 to 2014 at 10, 30, 60, 100 and 150 cm monitoring depths.

	1990 to 1993							2011 to 2014						
	Mean	Min	Max	Oxidizing[a]	Weakly reducing[b]	Moderately reducing[c]	Strongly reducing[d]	Mean	Min	Max	Oxidizing	Weakly reducing	Moderately reducing	Strongly reducing
	E_H / mV			/ %				E_H / mV			/ %			
10	547 ± 84[e]	377	761	98	2	0	0	562 ± 44	373	702	100	0	0	0
30	430 ± 137	28	739	75	23	0	0	573 ± 112	125	779	98	2	0	0
60	233 ± 273	–199	724	29	8	56	2	254 ± 293	–144	684	35	15	48	2
100	116 ± 221	–207	645	5	15	80	0	341 ± 199	81	702	31	46	23	0
150	–84 ± 171	–276	603	0	4	25	71	–184 ± 30	–243	–32	0	0	0	100

[a] E_H > 400 mV.
[b] E_H 400 to 200 mV.
[c] E_H 200 to –100 mV.
[d] E_H < –100 mV.
[e] Standard deviation.

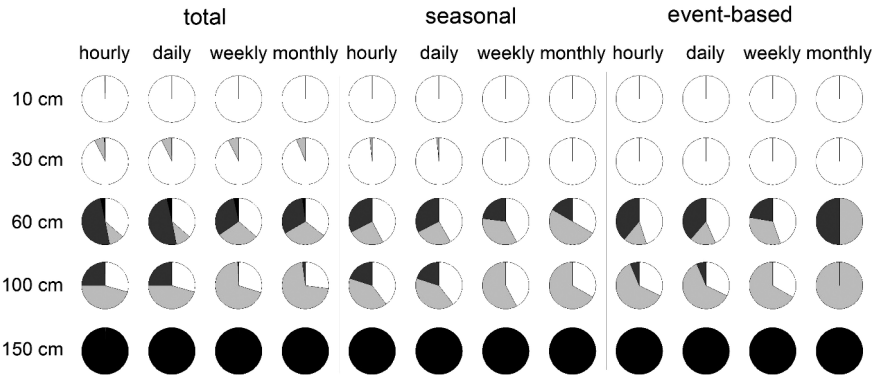

Figure 4: Comparison of the redox class distribution on an hourly, daily, weekly and monthly basis measurement intervals (columns) for the E_H recorded at depths of 10, 30, 60, 100, and 150 cm (lines) for the total (hydrological year 2011 to 2014), seasonal (hydrological summer 2011), and event-based (July and August 2012) time-scale. The pie charts display the percentage of oxidizing (> 400 mV; white), weakly reducing (400 mV to 200 mV; light grey), moderately reducing (200 mV to –100 mV; grey), and strongly reducing (< –100 mV; black) soil conditions according to *Zhi-Guang* (1985).

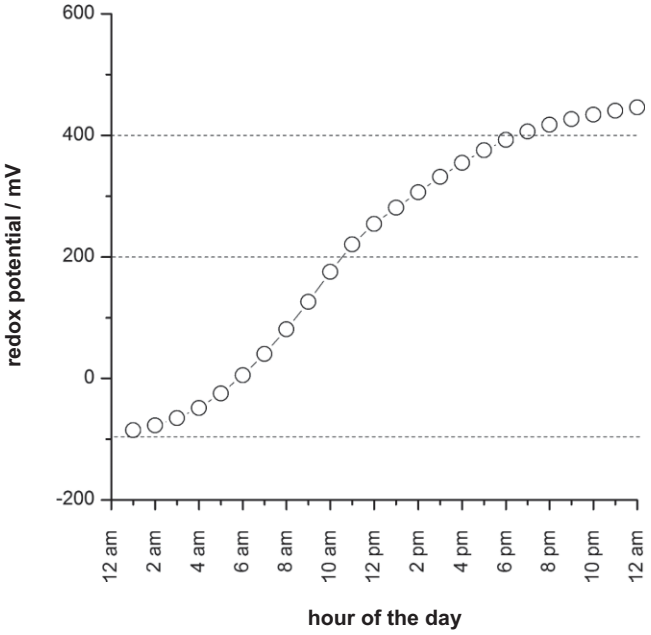

Figure 5: Redox potential (E_H) dynamics for a single platinum electrode at 60 cm depth on an hourly basis for a 24 h period on August 24, 2011. The dashed lines indicate the redox classes of oxidizing (> 400 mV), weakly reducing (400 mV to 200 mV), moderately reducing (200 mV to –100 mV), and strongly reducing (< –100 mV) soil conditions according to *Zhi-Guang* (1985).

namic. During the hydrological summers from 2011 to 2014, E_H increases at 60 and 100 cm depths occurred regularly, but with annual differences. The significance of temporal variation was particularly noticeable in August 2012 when the sharp decrease from 480 mV to 250 mV at 100 cm (Fig. 3i) was observed to be followed by a steep increase to 600 mV. Such variations in the E_H regime could easily be overlooked if only monthly readings are obtained. Even when weekly measurements are made, information about the temporal distribution between weakly and moderately reducing soil conditions would be lost at monitoring depths of 60 and 100 cm where WT fluctuations were present (Fig. 4). This indicates that these time intervals are not sufficient to derive trends of redox class distribution. Careful consideration should therefore be given to establishing a precise moment for measurement in the monitoring program (*e.g.*, for sampling of soil solution). Nevertheless, even daily E_H readings can be subject to shortcomings. Characterization of the soil redox status in the field at 7 am (40 mV) compared with 8 pm (420 mV) (Fig. 5), will lead to a faulty and misleading interpretation of the *in situ* biogeochemical conditions.

4.3 Redox potential measurements and implications for marsh soil development

The presence of sulfide minerals might alter the E_H reading by pushing the measured E_H values to more negative potentials when PtS is formed along the electrode tip surface (*Whitfield*, 1974). This theoretical limitation must be rejected for the study site, because sulfate-reducing bacteria require a readily available carbon source (*e.g.*, acetate as an electron donor), which was only present during the period of deposition of marine sediments and is no longer available at these depths. Hence, the diminishing of sulfide concentrations is a non-reversible process, even though SO_4^{2-} was detected at 150 cm depth at concentrations of up to 650 mg L^{-1} (*Mansfeldt*, 2004). It is assumed that elemental sulfur (S^0) formed during FeS oxidation at first remains at the mineral surface whilst soluble Fe^{2+} is subsequently leached into soil solution (*Nordstrom*, 1982). The measured E_H displays potentials driven by the redox couple FeS-S^0 (*Whitfield*, 1974). In this regard, a lowering of the FeS-containing Gr horizon from 105 to 135 cm might offer an explanation for why the mean E_H values from 1990 to 1993 (Fig. 3d) remain constantly below the E_H values from 2011 to 2014 at the 100 cm monitoring depth (Fig. 3i). The only proof of this assumption would be to continue monitoring of the E_H development at 150 cm to assess whether or not the E_H is altered by the decreasing *Protothionic* soil horizon over the next few years to decades. The CWB forecast

indicates that this process is likely to occur because the precipitation pattern and the PET_{Haude} indicate drier summers. The intensified WT drawdown would concur with prolonged periods of aeration in previously water-saturated soil environments (*Dorau* et al., 2015). *Picek* et al. (2000) demonstrated in laboratory soil incubation experiments that a change from reducing to oxidizing soil conditions results in elevated OC mineralization rates and enhanced CO_2 evolution, demonstrating the need to assess whether similar results are attained under field conditions during extended periods of aeration in the future. This process is not relevant for the study site by low OC contents but of relevance for other settings such as fens and bogs. Continuous monitoring of E_H by the use of permanently installed Pt electrodes is therefore of utmost importance in linking a change of environmental conditions to E_H development and *vice versa*.

5 Conclusions

A comprehensive understanding of biogeochemical processes in soils implies knowledge of the redox status. Soil chemical (OC content, FeS, pH) and physical properties (bulk density, porosity) have to be considered as a transient state within dynamic marsh ecosystems. As evident by this study, a linkage to E_H dynamics can only be achieved when Pt electrodes are placed permanently in the soil to differentiate whether variations of the E_H dynamics are either caused by the re-installation of the electrodes or by changes of soil properties. Redox potential measurements on an hourly and daily basis described the redox class distribution equally well during the study period from 2011 to 2014, but a loss of information occurred when weekly and monthly readings were performed. The findings demonstrate the need to measure E_H on an hourly basis, because fluctuations across three redox classes within 24 h were apparent. According to meteorological forecasts, enhanced evapotranspiration rates favor an intensified water table drawdown during the hydrological summer, which also results in prolonged periods of aeration and therefore extends the timeframe and extent for oxidizing soil conditions. This favors and accelerates topsoil compaction in marsh ecosystems and has implications for metastable minerals sensitive to oxidation.

Acknowledgments

This study was financially supported by *Verein der Freunde und Förderer der Universität zu Köln*. We kindly thank *Julian Rölkens* and *Marcel Possoch* for assistance during the sampling campaign in August 2013 and *Karin Greef* (University of Cologne) for support in the laboratory. Furthermore, *Dr. Stefan Wessel-Bothe*, ecoTech Bonn, is thanked for technical support. We thank two anonymous reviewer for their recommendations to improve the quality of the article.

References

AG Boden (2005): Bodenkundliche Kartieranleitung, 5th Ed. Schweizerbarth, Stuttgart, Germany.

Austin, W. E., *Huddleston, J. H.* (1999): Viability of permanently installed platinum redox electrodes. *Soil Sci. Soc. Am. J.* 63, 1757–1762.

Blume, H. P., *Müller-Thomsen, U.* (2007): A field experiment on the influence of the postulated global climatic change on coastal marshland soils. *J. Plant Nutr. Soil Sci.* 170, 145–156.

Brümmer, G., *Grunwaldt, H. S.*, *Schroeder, D.* (1971): Beiträge zur Genese und Klassifizierung der Marschen II. Zur Schwefelmetabolik in Schlicken und Salzmarschen. *Z. Pflanz. Bodenkunde* 129, 92–108.

Cornell, R. M., *Schwertmann, U.* (2003): The Iron Oxides: Structure, Properties, Reactions, Occurences and Uses. Wiley-VCH, Weinheim, Germany.

DeLaune, R. D., *Smith, C. J.*, *Patrick, W. H.* (1983): Relationship of marsh elevation, redox potential and sulfide to *Spartina alterniflora* productivity. *Soil Sci. Soc. Am. J.* 47, 930–935.

Dorau, K., *Gelhausen, H.*, *Esplör, D.*, *Mansfeldt, T.* (2015): Wetland restoration management under the aspect of climate change at a mesotrophic fen in Northern Germany. *Ecol. Eng.* 84, 84–91.

Faulkner, S. P., *Patrick, W. H.* (1992): Redox processes and diagnostic wetland soil indicators in bottomland hardwood forests. *Soil Sci. Soc. Am. J.* 56, 856–865.

Fiedler, S. (2000): In Situ Long-Term-Measurement of Redox Potential in Redoximorphic Soils, in Schüring, J., Schulz, H. D., Fischer, W. R., Böttcher, J., Duijnisveld, W. H. M. (eds.): Redox: Fundamentals, Processes and Applications. Springer, Heidelberg, Germany.

Fiedler, S., *Vepraskas, M. J.*, *Richardson, J. L.* (2007): Soil Redox Potential: Importance, Field Measurements and Observations, in Sparks, D. L. (ed.): Advances in Agronomy. Elsevier Academic Press Inc, San Diego, USA, pp. 1–54.

German Meteorological Service (2009): Daten der Klimastationen des Deutschen Wetterdienstes, Offenbach, Germany.

Gillespie, L. J. (1920): Reduction potentials of bacterial cultures and of water-logged soils. *Soil Sci.* 9, 199–216.

Glinski, J., *Stepniewski, W.* (1985): Soil Aeration and its Role for Plants. CRC Press, Boca Raton, USA.

Hoffmann, D. (1991): Sea level changes at the Schleswig-Holsteinian North Sea coast during the last 3000 years. *Quatern. Int.* 9, 61–65.

IUSS Working Group WRB (2014): World Reference Base for Soil Resources 2014. *World Soil Resources Reports*. 106, FAO, Rome, Italy.

Kuntze, H. (1986): Soil reclamation, improvement, recultivation and conservation in Germany. *Z. Pflanz. Bodenkunde* 149, 500–512.

Loepmeier, F. J. (1994): Berechnung der Bodenfeuchte und Verdunstung mittels agrarmeteorologischer Modelle. *Z. Bewässerun.* 29, 157–167.

Mansfeldt, T. (1993): Redoxpotentialmessungen mit dauerhaft installierten Platinelektroden unter reduzierenden Bedingungen. *Z. Pflanz. Bodenkunde* 156, 287–292.

Mansfeldt, T. (1994): Schwefeldynamik von Böden des Dithmarscher Speicherkoogs und der Bornhöveder Seenkette in Schleswig-Holstein. Schriftenreihe Institut für Pflanzenernährung und Bodenkunde 28. University of Kiel, Kiel, Germany.

Mansfeldt, T. (2003): In situ long-term redox potential measurements in a dyked marsh soil. *J. Plant Nutr. Soil Sci.* 166, 210–219.

Mansfeldt, T. (2004): Redox potential of bulk soil and soil solution concentration of nitrate, manganese, iron and sulfate in two Gleysols. *J. Plant Nutr. Soil Sci.* 167, 7–16.

Mansfeldt, T., *Blume, H. P.* (2002): Organic sulfur forms in mineral top soils of the marsh in Schleswig-Holstein, Northern Germany. *J. Plant Nutr. Soil Sci.* 165, 255–260.

Mehra, O. P., *Jackson, M. L.* (1960): Iron oxide removal from soils and clays by a dithionite-citrate system buffered with sodium bicarbonate. *Clay. Clay Miner.* 7, 317–327.

Müller-Ahlten, W. (1994a): Zur Genese der Marschböden. I. Der Einfluß von Sediment- und Bodengefüge. *Z. Pflanz. Bodenkunde* 157, 1–9.

Müller-Ahlten, W. (1994b): Zur Genese der Marschböden. II. Kalksedimentation, Entkalkung. *Z. Pflanz. Bodenkunde* 157, 333–343.

Nordstrom, D. K. (1982): Aqueous Pyrite Oxidation and the Consequent Formation of Secondary Iron Minerals, in Kittrick, J. A., Fanning, D. S., Hosner, L. R. (eds.): Acid Sulfate Weathering. Soil Science Society of America, Madison, USA, pp. 37–56.

Orlowsky, B., *Gerstengarbe, F. W.*, *Werner, P. C.* (2008): A resampling scheme for regional climate simulations and its performance compared to a dynamical RCM. *Theor. Appl. Climatol.* 92, 209–223.

Patrick, W. H., *Gambrell, R. P.*, *Faulkner, S. P.* (1996): Redox Measurements of Soils, in Sparks, D. L. (ed.): Methods of Soil Analysis: Chemical Methods, Part 3. Soil Science Society of America and American Society of Agronomy, Madison, USA, pp. 1255–1273.

Pfisterer, U., *Gribbohm, S.* (1989): Zur Herstellung von Platinelektroden für Redoxmessungen. *Z. Pflanz. Bodenkunde* 152, 455–456.

Picek, T., *Šimek, M.*, *Šantrůčková, H.* (2000): Microbial responses to fluctuation of soil aeration status and redox conditions. *Biol. Fert. Soil.* 31, 315–322.

Pillans, B. (1997): Soil development at snail's pace: evidence from a 6 Ma soil chronosequence on basalt in North Queensland, Australia. *Geoderma* 80, 117–128.

Ponnamperuma, F. N. (1972): The chemistry of submerged soils. *Adv. Agron.* 24, 29–96.

Potsdam Institute for Climate Impact Research (2013): STARS Klimaszenarien, Potsdam, Germany.

Reszkowska, A., *Krümmelbein, J.*, *Gan, L.*, *Peth, S.*, *Horn, R.* (2011): Influence of grazing on soil water and gas fluxes of two Inner Mongolian steppe ecosystems. *Soil Till. Res.* 111, 180–189.

Schroeder, D., *Brümmer, G.* (1969): Beiträge zur Genese und Klassifizierung der Marschen. I. Problematik der Marschen-Genese und -Klassifizierung und Untersuchungen zum Ca/Mg-Verhältnis. *Z. Pflanz. Bodenkunde* 122, 228–249.

Shoemaker, C., *Kroger, R.*, *Reese, B.*, *Pierce, S. C.* (2013): Continuous, short-interval redox data loggers: verification and setup considerations. *Environ. Sci.: Processes Impacts.* 15, 1685–1691.

Teichert, A., *Böttcher, J.*, *Duijnisveld, W. H. M.* (2000): Redox Measurements as a Qualitative Indicator of Spatial and Temporal Variability of Redox State in a Sandy Forest Soil, in Schüring, J., Schulz, H. D., Fischer, W. R., Böttcher, J., Duijnisveld, W. H. M. (eds.): Redox: Fundamentals, Processes and Applications. Springer, Heidelberg, Germany, pp. 95–109.

Vorenhout, M., *van der Geest, H. G.*, *van Marum, D.*, *Wattel, K.*, *Eijsackers, H. J. P.* (2004): Automated and continuous redox potential measurements in soil. *J. Environ. Qual.* 33, 1562–1567.

Whitfield, M. (1974): Thermodynamic limitations on the use of the platinum electrode in *Eh* measurements. *Limnol. Oceanogr.* 19, 857–865.

Wieder, R. K., *Lang, G. E.*, *Granus, V. A.* (1985): An evaluation of wet chemical methods for quantifying sulfur fractions in freshwater wetland peat. *Limnol. Oceanogr.* 30, 1109–1115.

Yang, J., *Hu, Y.*, *Bu, R.* (2006): Microscale spatial variability of redox potential in surface soil. *Soil Sci.* 171, 747–753.

Yu, K. W., *Wang, Z. P.*, *Vermoesen, A.*, *Patrick Jr., W. H.*, *Van Cleemput, O.* (2001): Nitrous oxide and methane emissions from different soil suspensions: effect of soil redox status. *Biol. Fert. Soil.* 34, 25–30.

Zhi-Guang, L. (1985): Oxidation-Reduction Potential, in Tian-Ren, Y. E. (ed.): Physical Chemistry of Paddy Soils. Springer, Berlin, Germany, pp. 1–26.

